Spatial coincidence of rapid inferred erosion with young metamorphic massifs in the Himalayas

David P. Finlayson
David R. Montgomery
Bernard Hallet

Quaternary Research Center and the Department of Earth and Space Sciences, University of Washington, Seattle, Washington 98195, USA

ABSTRACT

A spatially distributed rate-of-erosion index (EI) based on models of bedrock river incision documents a strong spatial correspondence between areas of high erosion potential and young metamorphic massifs as well as structural highs throughout the Himalayas. The EI is derived from slopes and drainage areas calculated from a hydrologically corrected digital elevation model (GTOPO30) combined with precipitation data (IIASA) to generate synthetic annual stream discharges. These variables drive three generalized process models to produce EI maps that, while differing in detail, provide an internally consistent, spatially continuous index of large-scale erosion rates. The large spatial variation in potential erosion rates in the Himalayas suggested by the EI patterns contrasts with the uniform convergence of the Indian subcontinent. If these EI gradients persist through time, they support the emerging view of a positive feedback between localized, rapid erosion and upward advection of lower crust.

Keywords: Himalayas, fluvial erosion, metamorphism, tectonics, maps.

INTRODUCTION

The eastern and western syntaxes of the Himalayas define the edges of the deformation front where India collides with Asia. The two largest rivers of the Himalayas abruptly end their respective courses paralleling the northern side of the range and turn south to cut two of the deepest gorges on Earth through the center of the syntaxes, transverse to the structural grain of the mountains. The sharp bends of these rivers and the steep gradients they exhibit throughout the syntaxial gorges are spatially correlated with young, metamorphic massifs (Burg et al., 1997; Zeitler et al., 2001) and, at least in the west where pertinent information is available, rapid fluvial incision (Burbank et al., 1996; Hancock et al., 1998). The close proximity of the rivers to the massifs together with high exhumation rates evident in the exposure of recently metamorphosed rocks, and a new tectonic model by Koons (1998), led Zeitler et al. (2001) to propose that tectonic and isostatic rock uplift beneath the erosional foci advects hot and therefore weak material from the mid-crust toward the surface, leading to a positive feedback in which rock uplift is locally accelerated, thereby producing and maintaining high topography in the face of rapid erosion.

This ''tectonic aneurysm'' model developed by Zeitler et al. (2001) raises two questions about the distribution of erosion in the Himalayas. First, if focused erosion centers exist, are they unique to particular areas or are they a common feature of the Himalayas? Second, do these erosional foci correspond spatially with the syntaxial areas where young metamorphic massifs occur? Answering these questions is straightforward only where sufficient data on contemporary erosion and long-term exhumation (comprising erosion and, potentially, tectonic exhumation) rates have been collected. There are erosion data for portions of the Indus (Burbank et al., 1996), the headwaters of the Ghandak (Galy, 1999) and the Sapt Kosi river basins (Lavé and Avouac,

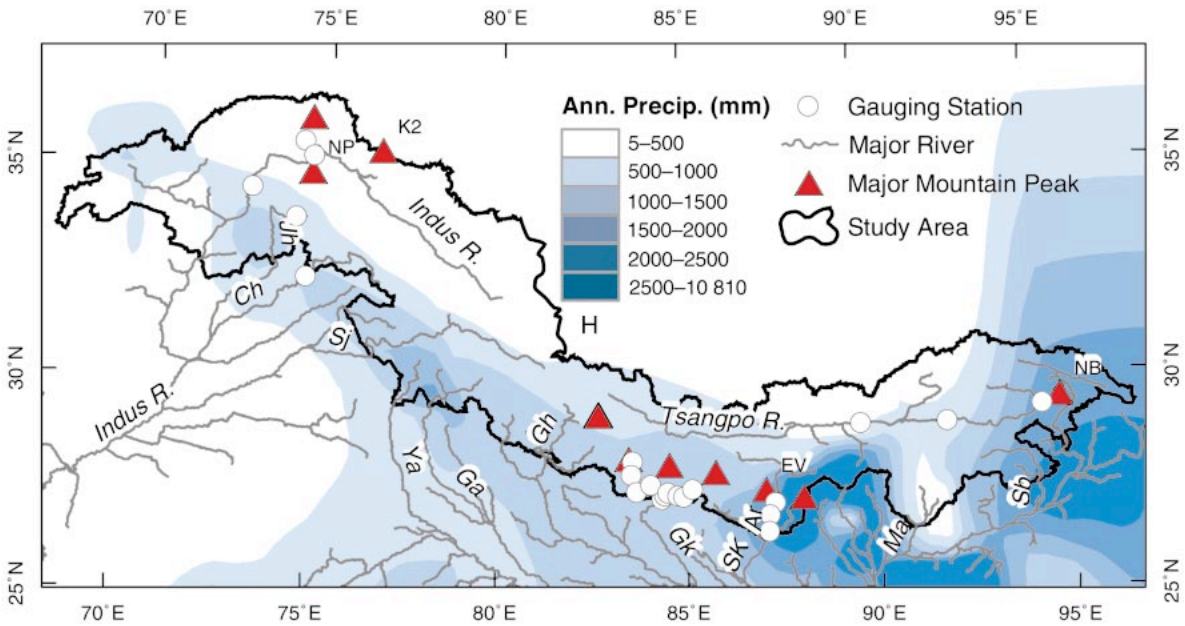

Figure 1. Annual net precipitation and model drainage network of the Himalayas. Net annual precipitation ranges from >10 m on southern flank of eastern syntaxis to <0.5 m on Tibetan Plateau. Synthetic river discharges were generated from this precipitation field and then calibrated against data from 21 gauging stations (shown) such that model discharge volumes of gauged channels matched measured discharges. Major rivers and mountain peaks are labeled for reference (Jh, Jhelum; Ch, Chenab; Sj, Sutlej; Ya, Yamuna; Ga, Ganga; Gh, Ghagra; Gk, Gandak; SK, Sapt Kosi; Ar, Arun; Ma, Manus; Sb, Subansiri; NP, Nanga Parbat; EV, Mount Everest; NB, Namcha Barwa).

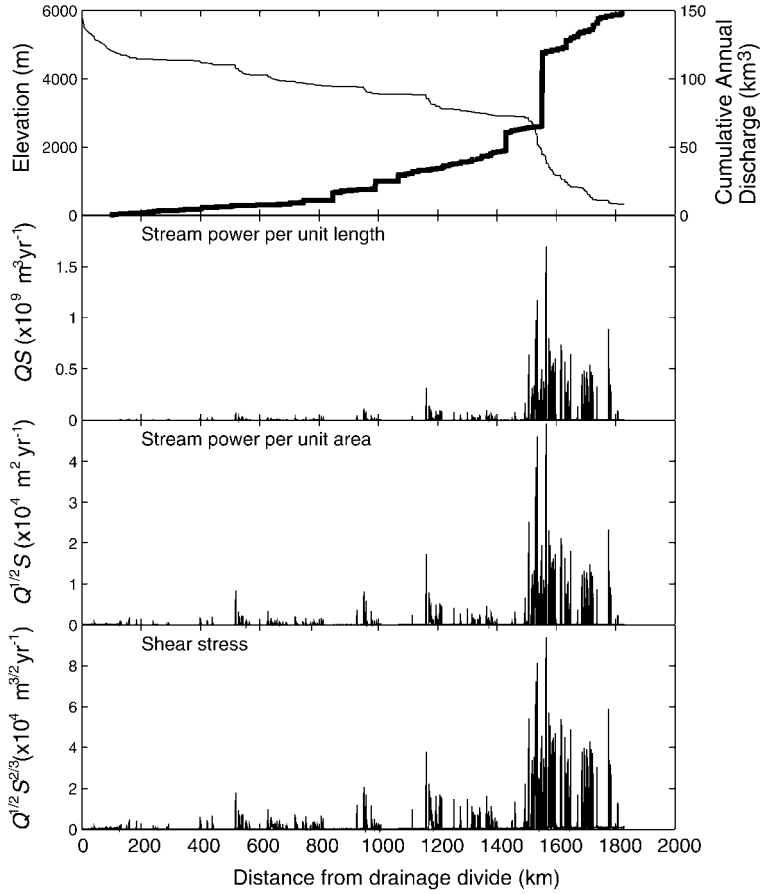

Figure 2. Modeled long profile of main-stem Tsangpo-Brahmaputra River from its drainage divide in southeastern Tibet down to where river crosses 250 m elevation contour at foot of Himalayas. Three variations of rate-of-erosion index (EI) calculated from synthetic mean annual discharge (*Q*) and local channel slope (*S*) are shown. Regardless of model chosen, EI is low on Tibetan Plateau where discharge and local slopes are relatively modest, and much higher as river enters gorge at eastern syntaxis and plunges to monsoon-drenched plains of Brahmaputra.

2000), and contemporary erosion rates averaged over the entire Himalayas have recently been estimated (Galy and France-Lanord, 2001). Nevertheless, information on the spatial pattern of exhumation and erosion rates is scarce for much of the Himalayas, in particular for the largest and potentially most erosive river, the Tsangpo-Brahmaputra; hereafter referred to as the Tsangpo. Furthermore, it is unlikely that detailed exhumation measurements will ever exist in sufficient quantities to permit the definition of detailed patterns of exhumation rates over broad areas. Consequently, in addressing the two questions posed here, we must capitalize on proxies of erosion rates that provide a spatially distributed index of erosion potential on the scale of the orogen. On the Indus River, there is evidence that bedrock river incision is coupled directly to basin-wide denudation through the undermining and failure of local mountain slopes (Burbank et al., 1996). Assuming that this is the general case throughout the Himalayas, we can examine the spatial pattern of fluvial erosion across the entire range and infer the regional exhumation pattern due to geomorphic processes. We use a fluvial erosion index (EI) to address the suggestion that spatial patterns of rapid erosion and active crustal upwelling tend to match one another throughout the Himalayas.

EROSION INDEX

We examine the spatial pattern of fluvial erosion rates across the Himalayas by applying the widely used stream power model and related models of bedrock incision by rivers to the Himalayan drainage network represented by the GTOPO30 digital elevation model (DEM) of Asia (U.S. Geological Survey, 1996). At the scale of this analysis, however, stream power, unit stream power, and shear stress are generalized abstractions of actual erosion processes. This type of abstraction should serve well as an erosion index in detachment limited regions and allow us to examine the spatial pattern of erosion in the Himalayas in a way that is impossible with individual denudation measurements.

Contemporary models of bedrock incision rate, $\dot{\epsilon}$, are typically cast as:

$$\dot{\epsilon} = KA^{m}S^{n}, \quad (1)$$

where A is the upstream contributing area (a proxy for discharge), S is channel slope (a proxy for the energy grade line of the channel), and K, m, and n are constants. Three different choices of m and n values represent river incision rates as functions of three distinct controls: total stream power (m = 1, n = 1), stream power per unit channel width (m = 1/2, n = 1), and shear stress (m = 1/2, n = 2/3) (Howard and Kerby, 1983; Whipple and Tucker, 1999). Values of K can vary over several orders of magnitude (Stock and Montgomery, 1999). Implicit in the stream power per unit channel width model is an assumed generic increase in river width, w, with discharge $w = aQ^{0.5}$ (where Q is effective discharge) an assumption that appears reasonable at least for data from bedrock channels in the western United States (Montgomery and Gran, 2001).

There are three basic assumptions in this family of erosion models: (1) that the coefficients and exponents are spatially uniform and temporally invariant (Whipple and Tucker, 1999), (2) that an effective discharge (Q) can be found that characterizes the flows responsible for channel incision (Whipple and Tucker, 1999), and (3) that precipitation is sufficiently uniform for A to constitute a suitable proxy for Q. This third assumption is inappropriate in the larger basins of the Himalayas, where river systems traverse from the arid expanses of the Tibetan Plateau (receiving as little as 0.1 m of rain per year) to the rain forests of northern India (receiving as much as 10 m of rain per year) (Fig. 1). In the case of the Tsangpo, the use of contributing area as a proxy for discharge significantly overestimates the increase in discharge along the portions of the river flowing over the dry Tibetan Plateau and grossly underestimates the increase in discharge of the river as it flows down the drenched flank of the Himalayas. To compensate for the discrepancy between contributing area and discharge, we modify the river incision relation to include discharge explicitly:

$$\dot{\epsilon} = KQ^{m}S^{n} = K\alpha \sum (AP)^{m}S^{n}, \quad (2)$$

where A and P represent the upstream area and net annual precipitation, respectively, and α is a parameter that can bring calculated annual net precipitation volumes of a subbasin into accord with gauged, annual discharge estimates. Modeling annual runoff volumes in this way, we calculate more precisely the in-

crease in discharge as rivers flow through different precipitation zones.

At the scale of the entire Himalayas we cannot expect to model erosion rates directly considering the lack of data on the spatial distribution of K values, which vary with channel characteristics (width, sediment cover), rock type, structure, and sediment transport rates (Sklar and Dietrich, 1998; Stock and Montgomery, 1999). Instead, we fold these local determinants of K into an erosion index, $EI = \dot{\epsilon}/K = \alpha\Sigma(AP)^m S^n$, which serves as an incision rate proxy in order to examine the broader scale potential for erosion in bedrock rivers. In separating the stream forcing portion of equation 2 from the resistance or susceptibility portion, K, the EI provides a direct index of relative erosion rates for the idealized case where the bedrock is uniformly resistant to fluvial erosion.

METHODOLOGY

The GTOPO30 DEM of Asia was clipped to include only the region encompassing the 16 major drainage basins of the Himalayas above 250 m elevation and projected onto a regular grid using a Lambert Conformal Conic Projection with a bilinear interpolation scheme. The resulting raster has a grid resolution of 853 m, covers a land area in excess of 2×10^6 km^2, and reproduces altitude, distance, and area measurements sufficiently well for regional analysis. We then followed standard filling and breaching procedures (Martz and Garbrecht, 1998) to create a hydrologically correct DEM of the Himalayas and southern Tibet from which we extracted local slopes and the river drainage network.

To model annual river discharge, we created an annual precipitation map from the IIASA Climate Database (Leemans and Cramer, 1991) and routed the water volume across the DEM using a precipitation-weighted flow accumulation in a standard algorithm (Jenson and Domingue, 1988). The resulting annual discharge volumes were compared to 22 gauging stations located throughout the Himalayas. In cases where there were discrepancies between the published and modeled annual discharge volumes at a gauge location, a correction factor, α, was applied to the IIASA data upstream of the gauge to lower or raise the river discharge until the model matched the published annual discharge volumes. However, we have no gauging data along many of the watersheds on the southern flank of the range. In these basins, we developed a generic α from data available on the upper Gandak (Galy, 1999), the Arun, and the Jhelum and Chenab Rivers (Collins, 1996), and then applied this generic factor ($\alpha = 1.43$) to all of the watersheds on the southern flank of the range. Overall, this modified precipitation-weighted flow-accumulation procedure accounts for spatial gradients in evapo-transpiration and differences in runoff-generation processes, while preserving the east-to-west gradient in the summer monsoon precipitation.

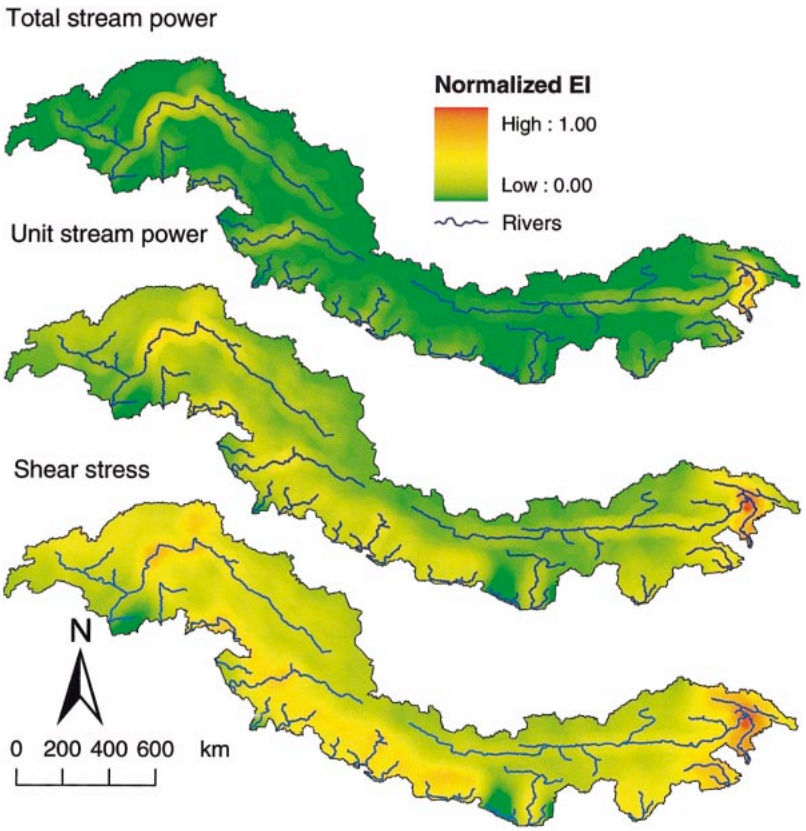

Figure 3. Relative potential for erosion across major watersheds of Himalayas. Each map represents a two-step process of calculating the rate-of-erosion index (EI) for every cell in the GTOPO30 digital elevation model (DEM) of the Himalayas and then passing a 50-km-radius moving average kernel over initial EI map. Final maps were colored by normalizing to maximum EI value for each model. Spatial pattern of EI does not change as much as magnitude of relative difference between locations. Regardless of model, EI of eastern syntaxis is greater than maximum values from other erosional foci. From top to bottom, EI model parameters were: $EI = QS$ (stream power per unit length), $EI = Q^{1/2}S$ (stream power per unit area), and $EI = Q^{1/3}S^{2/3}$ (shear stress), where Q is model discharge and S is DEM slope.

We calculated the EI of the Himalayas according to equation 2 using values of m and n to represent the stream power, unit stream power per channel width, and shear stress formulations of equation 1. To minimize the impact of spurious errors in the elevation data that affect local slopes, and thus EI values, and to facilitate comparison of regional patterns in erosion potential, the EI was calculated using two methods. The first method extracted river long profiles from the DEM and applied the EI models only to the main-stem channel (Fig. 2); the second method calculated the EI for every grid cell in the DEM and then a moving kernel averaged the EI potential of all cells within a 50 km radius (Fig. 3).

RESULTS

A typical profile for a trans-Himalayan river has its headwater in the Tibetan Plateau, cuts the High Himalaya through an impressive gorge, then plunges to the flood plains of the Indus and Ganges below. The spatial pattern of the erosion index on these rivers is closely tied to the gradient of the channel, and reveals a pattern of focused erosion centers along the southern flank of the Himalayas. To a large extent, the centers correspond to major river knickpoints (Seeber and Gornitz, 1983) and zones of extreme relief (Bilham et al., 1997; Bendick and Bilham, 2001) that define the arc of a small circle sweeping across the entire Himalayan chain.

The most dramatic example is the Tsangpo River (Fig. 2). From its headwaters in southern Tibet eastward 1500 km to the entrance of the gorge at Namcha Barwa, the river flows in the rain shadow of the High Himalayas across terrain of relatively low relief. After entering the gorge, the Tsangpo converges with the Po-Tsangpo River and the combined flow quickly descends from the plateau to the monsoon-drenched forests of northern India. In all three models, the EI are predictably low in

headwater reaches where both the discharge and gradient of the Tsangpo are modest, and increase dramatically when the river enters the gorge, particularly in the first 100 km. Here, the large discharge fueled by heavy monsoon precipitation combines with the extraordinary gradient of the river to produce exceptionally high EI values.

The three model results displayed in Figure 2 show that the specific formulation of the erosion law, with distinct m and n values representing different river incision process rules, affects the magnitude and variance of EI, but has a limited effect on its spatial pattern. The spiked nature of the EI reflects large, local changes in slope that are amplified by the very large discharges associated with these river systems.

The erosion index maps (Fig. 3) highlight distinct zones of high erosion potential associated with the steepest sections of the major rivers. Discrete erosion centers occur in both the syntaxes as well as in a number of central watersheds, notably those of the Subansiri and Sutlej Rivers. On the Indus River, two zones of high EI are apparent; the first is at the western syntaxis near Nanga Parbat, and the second is downstream of Chilas. The most significant zone of elevated erosion potential is the eastern syntaxis (Tsangpo), where average EI estimates are 1.4 (shear stress) to 3.7 (stream power) times greater than the next largest zone in the Indus gorge. The difference in the range of EI values between the three models changes the importance of the central rivers channels relative to the syntaxial gorges (leading to the contrast in the patterns of the three models in Fig. 3) but does not change where rapid fluvial erosion is most likely to be occurring in the orogen. One caution in the interpretation of Figure 3 is that high EI values are found only within the river channels, while the adjacent hillslopes have EI values several orders of magnitude smaller. The smoothing applied to Figure 3 exaggerates the areal extent of EI patterns so that these patterns can be visualized at this small scale.

DISCUSSION

Even simple models such as the EI serve an important first-order role in geomorphic modeling. Although we do not know how rock resistance, K, varies throughout the range, it would take a pattern equally strong in K (and all else that K represents) to counter the EI pattern shown in Figure 3. Both the eastern and western syntaxes are localized zones of high erosion potential and both have been identified as regions of young metamorphic massifs and active crustal aneurysms (Zeitler et al., 2001). In addition, other locations lower in the Indus drainage, and along the Sutlej and Subansiri Rivers, have high EI values, and hence merit further investigation.

High EI values (particularly those predicted by the shear stress model shown in Fig. 3) also appear to be coincident with the transverse anticlines (~10 km amplitude) reported on the Arun, Karnali and other Nepalese river drainages (Oberlander, 1985). Oberlander (1985) preferred to attribute these "river anticlines" to tectonics and drainage antecedence. However, our analysis points to a link between erosional and structural development along these valleys that is similar to that underlying crustal aneurysms in the syntaxes. Assuming that rates of bedrock erosion and long-term exhumation correlate with the erosion index, there is a rich spatial complexity in the rates of erosion and evacuation of material from the range that contrasts with the uniform convergence of crustal material into the orogen due to northward motion of the Indian subcontinent (Bilham et al., 1997; Bendick and Bilham, 2001). This apparent spatial disparity between input and output of material from the Himalayas challenges our understanding of how topography in this and similar ranges arises and is maintained from the interactions of tectonic and geomorphic processes.

ACKNOWLEDGMENTS

We thank Adarsha P. Pokhrel, Director General, and Birbal Rana of the Department of Hydrology and Meteorology of Nepal for generously providing us discharge data for the Arun River; and Robert Anderson, Peter Koons, and Peter Molnar for constructive reviews. The final phase of this work was supported by the National Science Foundation (EAR-0003561) and NASA (NAG 5-10342).

REFERENCES CITED

Bendick, R., and Bilham, R., 2001, How perfect is the Himalayan arc?: Geology, v. 29, p. 791–794.

Bilham, R., Larson, K.M., Freymueller, J.T., and Project Idylhim Members, 1997, GPS measurements of present-day convergence across the Nepal Himalaya: Nature, v. 386, p. 61–63.

Burbank, D.W., Leland, J., Fielding, E., Anderson, R.S., Brozovic, N., Reid, M.R., and Duncan, C., 1996, Bedrock incision, rock uplift and threshold hillslopes in the northwestern Himalayas: Nature, v. 379, p. 505–510.

Burg, J.P., Davy, P., Nievergelt, P., Oberli, F., Seward, D., Diao, Z., and Meier, M., 1997, Exhumation during crustal folding in the Namcha Barwa syntaxis: Terra Nova, v. 9, p. 117–123.

Collins, D.N., 1996, Sediment transport from glacierized basins in the Karakoram Mountains, *in* Walling, D.E., and Webb, B., eds., Erosion and sediment yield: Global and regional perspectives: International Association of Hydrological Sciences Publication 236, p. 85–96.

Galy, A., 1999, Etude géochimique de l'érosion actuelle de la chaîne Himalayenne, [Ph.D. thesis]: Lorraine, l'Institut National Polytechnique de Lorraine, 475 p.

Galy, A., and France-Lanord, C., 2001, Higher erosion rates in the Himalaya: Geochemical constraints on riverine fluxes: Geology, v. 29, p. 23–26.

Hancock, G.S., Anderson, R.S., and Whipple, K.X., 1998, Beyond power: Bedrock river incision process and form, *in* Tinkler, K.J., and Wohl, E.E., eds., Rivers over rock: Fluvial processes in bedrock channels: American Geophysical Union Geophysical Monograph 107, p. 35–60.

Howard, A., and Kerby, G., 1983, Channel changes in badlands: Geological Society of America Bulletin, v. 94, p. 739–752.

Jenson, S.K., and Domingue, J.O., 1988, Extracting topographic structure from digital elevation data for geographic information systems analysis: Photogrammetric Engineering and Remote Sensing, v. 54, p. 1593–1600.

Koons, P.O., 1998, Big mountains, big rivers, and hot rocks; beyond isostasy [abs.]: Eos (Transactions, American Geophysical Union), v. 79, no. 45, supplement, p. F908.

Lavé, J., and Avouac, J.P., 2000, Active flooding of fluvial terraces across the Siwaliks hills, Himalayas of central Nepal: Journal of Geophysical Research, v. 105, p. 5735–5770.

Leemans, R., and Cramer, W.P., 1991, The IIASA database for mean monthly values of temperature, precipitation and cloudiness of a global terrestrial grid: Laxenburg, Austria, International Institute for Applied System Analyses Publication RR-91-18, 62 p.

Martz, L.W., and Garbrecht, J., 1998, The treatment of flat areas and depressions in automated drainage analysis of raster digital elevation models: Hydrological Processes, v. 12, p. 23–36.

Montgomery, D.R., and Gran, K.B., 2001, Downstream hydraulic geometry of bedrock channels: Water Resources Research, v. 37, p. 1841–1846.

Oberlander, T.M., 1985, Origin of drainage transverse to structures in orogens, *in* Morisawa, M., and Hack, J.T., eds., Tectonic geomorphology: New York, Allen & Unwin, p. 155–182.

Seeber, L., and Gornitz, V., 1983, River profiles along the Himalayan arc as indicators of active tectonics: Tectonophysics, v. 19, p. 335–367.

Sklar, L., and Dietrich, W., 1998, River longitudinal profiles and bedrock incision models: Stream power and the influence of sediment supply, *in* Tinkler, K.J., and Wohl, E.E., eds., Rivers over rock: Fluvial processes in bedrock channels: American Geophysical Union Geophysical Monograph 107, p. 237–260.

Stock, J., and Montgomery, D.R., 1999, Geologic constraints on bedrock river incision using the stream power law: Journal of Geophysical Research, v. 104, p. 4983–4993.

U.S. Geological Survey, 1996, GTOPO30 global digital elevation model: Sioux Falls, South Dakota, EROS Data Center.

Whipple, K.X., and Tucker, G.E., 1999, Dynamics of the stream-power river incision model: Implications for height limits of mountain ranges, landscape response timescales, and research needs: Journal of Geophysical Research, v. 104, p. 17 661–17 674.

Zeitler, P.K., Meltzer, A.M., Koons, P.O., Craw, D., Hallet, B., Chamberlain, C.P., Kidd, W.S.F., Park, S., Seeber, L., Bishop, M., and Shroder, J., 2001, Erosion, Himalayan geodynamics and the geomorphology of metamorphism: GSA Today, v. 11, no. 1, p. 4–9.

Manuscript received May 24, 2001
Revised manuscript received October 22, 2001
Manuscript accepted November 19, 2001

Printed in USA